Research Square

Preprints are preliminary reports that have not undergone peer review.
They should not be considered conclusive, used to inform clinical practice,
or referenced by the media as validated information.

TRIB2 sustains MITF-dependent differentiated phenotype and associates with resistance to immune checkpoint inhibitors in melanoma

Wolfgang Link

walink@iib.uam.es

Instituto de Investigaciones Biomédicas https://orcid.org/0000-0002-3340-5165

Andrés de la Rocha-Muñoz

IIBM

Alba Orea-Soufi

IIBM

Alicia Ruiz Martí

IIBM

Ignacio Vaquero Marín

IIBM

Sara de la Calle Santiago

IIBM

Bibiana Ferreira

María Jesús Martin-Bermejo

CSIC

Paola Bovolenta

Antonio Barbachano

CSIC

Asunción Fernández-Barral

Instituto de Investigaciones Biomédicas Sols-Morreale https://orcid.org/0000-0002-1278-4645

Lucía Jiménez

IIBM

Article

Keywords:

Posted Date: October 22nd, 2026

DOI: https://doi.org/10.21203/rs.3.rs-11077066/v1

License: This work is licensed under a Creative Commons Attribution 4.0 International License.
Read Full License

Additional Declarations: (Not answered)

Abstract

Melanoma plasticity, driven by dynamic switching between differentiated and dedifferentiated cell states, contributes to tumor heterogeneity, disease progression and resistance to immune checkpoint inhibitors. Tribbles pseudokinase 2 (TRIB2) is an oncogenic protein overexpressed in melanoma and has been associated with disease progression, but its exact role remains poorly understood. Here, we integrated TCGA skin cutaneous melanoma bulk RNA-seq data, two anti-PD1 immunotherapy cohorts and scRNA-seq data from metastatic melanoma to characterize the transcriptomic landscape of TRIB2, and functionally validated our findings using a CRISPR-Cas9-generated TRIB2 knockout melanoma cell model. TRIB2 expression positively correlated with melanocyte differentiation/pigmentation genes and negatively correlated with cytokine- and lymphocyte-related genes; at single-cell resolution, TRIB2 was highest in malignant cells relative to most non-malignant tumor microenvironment populations. Mechanistically, TRIB2 positively correlated with microphthalmia-associated transcription factor (MITF) and its melanogenic target genes, and TRIB2 KO cells showed reduced MITF and melanogenic gene/protein expression together with impaired fibronectin adhesion. TRIB2 also positively correlated with CTNNB1/β-catenin and negatively with WNT5A, and TRIB2 KO cells showed decreased β-catenin and increased WNT5A/NFATC2 levels. This effect persisted after pharmacological activation of canonical WNT/β-catenin signaling, which induced a stronger melanogenic response in WT than KO cells. Unsupervised clustering based on this signature stratified melanoma patients into two groups, identifying a subgroup with worse overall survival characterized by high TRIB2, MITF and CTNNB1, and reduced WNT5A and CD8+ T cell-related gene expression. TRIB2 negatively correlated with a CD8+ T cell gene signature and was elevated in tumors from patients without clinical benefit from anti-PD1 therapy, with reduced expression on-treatment in responders. These findings identify TRIB2 as a regulator of melanoma cell plasticity that sustains an MITF-dependent, β-catenin-driven differentiated phenotype, and as a candidate contributor to immune exclusion, supporting further investigation of TRIB2 as a prognostic biomarker or therapeutic target to improve ICI response in melanoma.

Introduction

Melanoma is a malignant neoplasm of increasing incidence with aggressive behavior and high metastatic potential [1]. Although the development of targeted therapies and immune checkpoint inhibitors (ICI) has significantly enhanced the therapeutic landscape, melanoma remains a major global public concern, as approximately half of patients with advanced disease die within 5 years [2]. A major challenge underlying therapy is the heterogeneity and plasticity of melanoma biology, which allow tumors to adapt and eventually become resistant to the most advanced treatments [3].

This plasticity is explained by the phenotype switching model. According to it, malignant cells, stimulated by extracellular factors from the tumor microenvironment (TME), dynamically transition between a more differentiated, proliferative state and a less differentiated, invasive phenotype through multiple intermediate states that combine features of both phenotypes [4]. Importantly, this switching is

accompanied by extensive remodelling of the TME, including changes in $CD8^+$ cytotoxic T cell infiltration and activity, a major determinant of response to ICI [5]. Therefore, melanoma plasticity promotes not only tumor growth and metastasis, but also contributes to resistance to therapy with ICI [6].

At the molecular level, phenotype switching is governed by microphthalmia-associated transcription factor (MITF), a lineage transcription factor critical for melanocyte differentiation, proliferation, and survival [7]. MITF, along with the expression of melanogenic genes, is tightly associated to the differentiated phenotype and seems to act as a gatekeeper for the transition to the invasive state [8,9]. However, the molecular mechanisms underlying phenotype switching are highly complex and involve the coordination of multiple signaling networks beyond the MITF transcription program. Among them, the WNT signaling pathways have emerged as key regulators of melanoma plasticity [10]. By controlling MITF-dependent melanocytic commitment, cytoskeletal reorganization, and cellular motility, canonical WNT/β-catenin and non-canonical WNT/Ca^{2+} signaling underlie the differentiated and dedifferentiated phenotypes, respectively [11]. Importantly, beyond its role in melanoma cell-state regulation, β-catenin signaling has also been implicated in $CD8^+$ T cell exclusion and resistance to immune checkpoint blockade [12].

Tribbles pseudokinase 2 (TRIB2) is a member of the Tribbles family of serine/threonine pseudokinases, characterized by their ability to act as molecular scaffolds and regulators of protein degradation [13,14]. Through the interaction with its downstream partners, TRIB2 plays a key role in cellular processes such as proliferation, senescence, stem cell pluripotency, immune response, or cell survival [15]. In cancer, a multifunctional role of TRIB2 as an oncogenic protein has been described across hematological and solid malignancies including leukemia, pancreatic, liver, ovarian and lung cancer [16-20]. In the context of melanoma, our laboratory has previously demonstrated that TRIB2 expression is elevated in these tumors, particularly in metastatic disease, and has proposed TRIB2 as a biomarker for diagnosis and prognosis [21]. However, despite this clinical association, the specific oncogenic processes regulated by TRIB2 in melanoma, and their broader clinical relevance, remain poorly characterized.

Here, we combined analyses of bulk- and single-cell RNA-sequencing (scRNA-seq) datasets from melanoma tumors and functional studies in a CRISPR-generated TRIB2 knockout (KO) melanoma cell model to investigate the role of TRIB2 in melanoma biology. We show that TRIB2 sustains a differentiated phenotype associated to the MITF-dependent melanogenic program, β-catenin signaling and suppression of WNT5A/NFATC2. Importantly, TRIB2 expression is closely associated with reduced $CD8^+$ T cell gene expression and with resistance to ICI therapy. These findings identify TRIB2 as a regulator of melanoma cell plasticity and a candidate driver of immune exclusion, with potential clinical relevance for immunotherapy response.

Methods

Publicly available datasets

Bulk RNA-seq data from the TCGA Skin cutaneous melanoma (TCGA-SKCM) cohort (dataset: TCGA.SKCM.sampleMap/HiSeqV2; IlluminaHiSeq, log2[norm_count+1] normalized values) and the corresponding clinical survival annotations (survival/SKCM_survival.txt) were downloaded from the UCSC Xena browser (https://xenabrowser.net). scRNA-seq data from metastatic melanoma tumors reported by Jerby-Arnon et al. (2018) [22] (dataset: melanoma_Jerby-Arnon/tumors_tpm.txt, n = 7,186 cells; originally deposited at the Broad Single Cell Portal, SCP109, and GEO accession GSE115978), together with the corresponding cell-type and treatment annotations, were obtained from the Xena single-cell hub, with gene expression reported as log2(TPM+1). The melanoma immunotherapy cohort from Liu et al. (2019) [23] was obtained from cBioPortal as the CRI iAtlas-harmonized subset of this cohort (study ID: mel_iatlas_liu_2019; n = 122 of the original 144 patients), together with the corresponding clinical benefit annotations. The melanoma immunotherapy cohort from Riaz et al. (2017) [24] was obtained from the Gene Expression Omnibus (GEO; accession GSE91061, file GSE91061_norm_counts_TPM_GRCh38.p13_NCBI.tsv.gz), whereas the corresponding pre-/on-treatment and response annotations were obtained from Table S2 of the original publication.

Correlation analysis and functional enrichment

Pearson correlation coefficients between TRIB2 expression and all expressed genes in the TCGA-SKCM cohort were calculated using the cor.test function in R (v4.3.0) using RStudio. P values were adjusted for multiple testing using the Benjamini–Hochberg false discovery rate (FDR) method. Genes with Pearson correlation coefficients greater than 0.3 or lower than −0.3 were defined as the top positively and negatively correlated genes with TRIB2, respectively. All genes meeting these correlation thresholds were statistically significant after FDR correction (FDR < 0.05).

Gene Ontology (GO) Biological Process enrichment analyses were performed separately for the positively and negatively correlated gene sets using the clusterProfiler package, after converting gene symbols to Entrez Gene identifiers with the org.Hs.eg.db annotation package. GO terms were ranked according to their Benjamini–Hochberg-adjusted P values (p.adjust), and the five most significantly enriched Biological Process terms were selected for visualization.

Unsupervised clustering

The expression matrix comprising TRIB2 together with the top positively and negatively correlated genes in TCGA-SKCM was centered and scaled prior to unsupervised K-means clustering (k = 2, 25 random starts, maximum of 100 iterations). Principal component analysis (PCA) was subsequently performed on the scaled expression matrix using the prcomp function to visualize sample distribution across clusters.

Survival analysis

Overall survival analyses were performed by integrating cluster assignments with the corresponding TCGA-SKCM clinical annotations. Kaplan–Meier survival curves were generated using the survival and survminer R packages, and differences between groups were assessed using the log-rank test.

Analysis of immunotherapy cohorts

TRIB2 expression was evaluated in two independent melanoma immunotherapy cohorts with distinct study designs. In the Liu et al. (2019) cohort, TRIB2 expression was compared in pre-treatment tumor samples between patients with and without clinical benefit from anti-PD1 therapy. In the Riaz et al. (2017) cohort, TRIB2 expression was assessed in matched tumor samples collected before treatment and during anti-PD1 therapy, separately in responders and non-responders. Normalized gene expression matrices (TPM) were used to extract TRIB2 expression values, which were matched to the clinical annotations provided with each dataset.

Cell lines

UACC-62 cells were purchased from American Type Culture Collection (ATCC, Manassas, VA, USA.). All UACC-62 cell lines were grown at 37 °C and 5% CO_2 in DMEM high glucose (Cytiva, Marlborough, MA, USA) supplemented with 10% fetal bovine serum (FBS) and penicillin/streptomycin (PanReac Applichem, Castellar del Vallès, Spain). As standard procedure, all cell lines were periodically tested for mycoplasma contamination. UACC-62 TRIB2 KO clones (KO#28 and KO#31) cells were developed by CRISPR/Cas9 technology as described previously [25]. Briefly, after cells were transfected with two independent guide RNAs in plasmid vectors expressing Cas9 nuclease protein, single-cell clones were selected and expanded. Finally, the full deletion of the protein levels of TRIB2 was evaluated by WB.

Quantitative real-time PCR (qPCR)

Total RNA was extracted from samples following the NucleoSpin RNA Plus (Macherey-Nagel, Düren, Germany.). cDNA was synthetized using the High Capacity cDNA Reverse Transcription kit and qPCR was performed on 7900HT Fast Real Time PCR using SYBR Green Master Mix (all from Thermo Fisher Scientific, Waltham, MA, USA). Relative gene expression levels were quantified by the $2^{-\Delta\Delta Ct}$ method using glyceraldehyde-3-phosphate dehydrogenase (GAPDH) as housekeeping gene.

Protein extraction and western blotting

UACC-62 cells were lysed in RIPA buffer supplemented with phosphatase and protease inhibitors. Protein concentration was determined by BCA assay (Thermofisher-Scientific). Then, samples were mixed with Laemmli buffer and heated at 95 °C for 5 min. Proteins lysates were separated by SDS-PAGE using 10% resolving gels and transferred to PVDF membranes with a semi-dry transfer system. Membranes were blocked in Tris-buffered saline with 0.1% Tween 20 detergent (TBS-T) containing 5% non-fat milk or 5% bovine serum albumin (BSA) for 1 h at RT. After that, membranes were incubated overnight at 4°C with primary antibodies diluted in TBS-T containing 5% non-fat milk or 5% BSA. After washing with TBS-T buffer, membranes were incubated for at least 1 h with the respective secondary antibodies at the appropriate dilutions. Protein bands were detected by ECL (Cytiva RPN3244), imaged using a Fusion FX6 system and quantified using Evolution-Capt Edge software (both from Vilber, Collégien, France).

Primary antibodies were as follows: anti-TRIB2 D8P2X (1:1000, Cell Signaling Technology, Danvers, MA, USA, #13533), anti-MITF D5G7V (1:2000, Cell Signaling Technology, #12590), anti-β-catenin E247 (1:1000, Abcam, Cambridge, UK, ab32572), anti-NFATC2 (1:1000, BD Transduction Laboratories, Lexington, KY, USA, 610702), anti-SFRP1 (1:500, Cell Signaling Technology, #4690), anti-α-tubulin (1:10000, Merck, Darmstadt, Germany, T9026), anti-β-actin AC-15 (1:20000, Sigma-Aldrich, St. Louis, MO, USA, A5441) and anti-lamin A/C 4C11 (1:1000, Cell Signaling Technology, #4777) HRP-conjugated secondary antibodies included mouse anti-rabbit IgG-HRP (1:5000, Santa Cruz Biotechnology, Dallas, TX, USA, sc-2357) and m-IgGκ BP-HRP (1:3000, Santa Cruz Biotechnology, sc-516102).

Immunofluorescence

Cells seeded on glass coverslips were washed with PBS prior to fixation with paraformaldehyde (PFA) 4% for 10 min. After washing with PBS, cells were permeabilized with PBS containing 1% BSA and 0.1% Triton X-100 for 10 min. Non-specific binding was blocked for 1 h with PBS containing 0.1% BSA and incubated overnight at 4 °C with anti-β-catenin E247 (1:200) in blocking solution. The following day, cells were washed several times with PBS and incubated for 1 h with Alexa Fluor 488-conjugated anti-rabbit secondary antibody (1:200) and DAPI (1:500) (both from Thermo Fisher Scientific) in blocking solution. Finally, cells were washed, mounted using ProLong Gold Antifade Mountant (Thermo Fisher Scientific) and stored at 4 °C. Images were acquired using a Nikon Eclipse 90i fluorescence microscope equipped with a DS-QiMc camera (Nikon, Nishi-Ōi, Japan). Cells were imaged under identical imaging conditions and fluorescence was quantified using ImageJ software.

Fibronectin adhesion assays

Glass coverslips were coated with fibronectin (Sigma-Aldrich) at 10 µg/mL and incubated overnight at 4 °C in a humidified chamber, followed by transfer into 24-well plates. UACC-62 cells were seeded onto fibronectin-coated coverslips and allowed to adhere for 1 h at 37 °C. Cells were then fixed with 4% PFA for 15 min, washed with 1X PBS, and permeabilized with 0.1% Triton X-100 in PBS for 10 min. Nuclei were stained with DAPI for 20 min in the dark, followed by a final PBS wash. Coverslips were mounted onto glass slides using ProLong Gold Antifade Mountant. Images were acquired on a Nikon Eclipse 90i fluorescence microscope equipped with a DS-QiMc camera (Nikon) using NIS-Elements software, and analyzed using ImageJ software.

Pharmacological treatments

For inducing WNT/β-catenin activation, UACC-62 cells were incubated for 48 h with conditioned media containing WNT3A or the GSK3β inhibitor CHIR98014 (Selleck Chemicals, Houston, TX, USA) at 1 µM. WNT3A-conditioned medium was generated using L-Wnt3a cells. Cells were maintained in DMEM supplemented with 8 % FBS and selected with the antibiotic geneticin G418 (600 µg/mL; InvivoGen, San Diego, CA). After three days, cells were seeded into T175 flasks at a density of 2.5×10^6 cells/flask and cultured in DMEM containing 8 % FBS. Four days later, the conditioned medium was harvested and replaced with fresh medium. Following an additional three days of culture, a second batch of conditioned

medium was collected and pooled with the first. The combined medium was centrifuged to remove cellular debris, sterile-filtered, aliquoted, and stored at −20 °C until use.

For the inhibition of SFRP1, UACC-62 were incubated with BML-287 at concentrations ranging from 30 to 100 μM (Enzo Live Sciences, Farmingdale, NY, USA, kindly provided by Paola Bovolenta, CBMSO) at the indicated concentrations for 48 h. Intracellular accumulation of SFRP1 in UACC-62 cells was induced by 4 h treatments with 5 μg/mL of Brefeldin A (Sigma-Aldrich).

Data analysis and statistics

All data and statistical analyses were performed using GraphPad Prism (GraphPad Software, San Diego, CA, USA). Kruskal–Wallis or ordinary one-way ANOVA tests were used to compare multiple groups, with subsequent Dunn's or Holm-Šídák's post hoc tests to determine significant differences between samples. Two-way ANOVA was used to assess the combined effect of two independent variables (e.g., genotype and treatment) and their interaction, followed by Dunnett's multiple comparisons test. Mann–Whitney U test was used to compare two separate groups.

P values are denoted through the text as follows: *$p < 0.05$; **$p < 0.01$; ***$p < 0.001$; ****$p < 0.0001$; $p <$ 0.05 or lower values were considered significantly different.

Results

TRIB2 is linked to differentiation and immune-related transcriptional programs in melanoma

To investigate the biological processes associated with TRIB2 in melanoma, we analyzed the transcriptomic landscape associated to TRIB2 using the TCGA-SKCM bulk RNA-seq dataset (Fig. 1A). We first performed Pearson correlations between the expression of TRIB2 and the rest of 20 529 genes available in the dataset. As a result, TRIB2 showed moderate-strength Pearson correlations across the transcriptome, with r values ranging from −0.38 to 0.47 (Fig. 1B). Importantly, 6 734 genes correlated significantly (FDR < 0.05) with TRIB2; 2 885 positively and 3 849 negatively (Supplementary material 1). Based on the magnitude of the Pearson correlation coefficient, genes with r > 0.3 or r < −0.3 were considered the top positively and negatively correlated genes with TRIB2, respectively. Using these thresholds, we found 137 genes above the r > 0.3 cutoff and 100 genes below the r < -0.3 cutoff (Supplementary material 1). To assign functional meaning to these genes, we conducted a GO Pathway Enrichment Analysis on the lists of top positively and top negatively co-expressed genes (Fig. 1A). As shown in Figures 1C, the top GO terms for positively correlated genes were related to melanocyte differentiation and pigmentation, while those for negatively correlated genes were related to cytokine signaling and lymphocyte/leukocyte regulation.

Given that both differentiation- and immune-related processes emerged from bulk-level analysis, we next asked whether TRIB2 expression was specifically enriched in malignant cells or broadly distributed across the tumor microenvironment, leveraging the publicly available scRNA-seq dataset from Jerby-

Arnon et al. (2018) [22]. Specifically, we followed a pseudobulk approach, averaging TRIB2 expression across cells of each population within every tumor and retaining, for each cell type, only tumors with at least 10 profiled cells of that type (Fig. 1D). As a result, analyses showed that malignant cells displayed the highest TRIB2 expression among all annotated cell types, with significant differences relative to infiltrating immune cells, but not relative to endothelial cells (Fig. 1E).

Altogether, these findings suggest that TRIB2 expression is associated to two specific transcriptional programs in melanoma, melanocyte differentiation and immune activity, and that this association is largely intrinsic to malignant cells rather than driven by differences in immune cell composition across tumors.

TRIB2 controls MITF and the melanogenic gene expression program in melanoma

The above observations position TRIB2 as a candidate regulator of both melanoma cell identity and the tumor immune microenvironment, prompting us to next investigate its mechanistic role in sustaining the differentiated phenotype. Melanocyte differentiation, a process of high clinical relevance in melanoma, is governed by the melanocytic transcription factor MITF [7]. Thus, MITF emerged as a potential link between TRIB2 and the differentiation program.

We therefore examined the correlation between TRIB2 and MITF, as well as several MITF target genes, in the TCGA-SKCM dataset. Among target genes, we included genes related to melanogenesis (MLANA, TYR, TYRP1, DCT), survival (BCL2, BCL2A1) and cell cycle (CDK2, CDK4, CDKN2A). As shown in Fig. 2A, TRIB2 showed a moderate-strength positive correlation with MITF and weak-to-moderate positive correlations with each of the remaining MITF target genes assessed, all of which reached statistical significance (at least, $p < 0.05$). No significant correlation was observed for CDKN2A. As complementary analyses, significant positive correlations between TRIB2 and MITF melanogenic target genes were also found in the Liu et al. (2019) and Riaz et al. (2017) bulk RNA-seq datasets, as well as in malignant cells from tumors included in the Jerby-Arnon et al. (2018) scRNA-seq dataset (Supplementary Fig. 1).

Next, to establish a causal role for TRIB2 in regulating MITF and the melanocytic differentiation program, we leveraged the TRIB2 KO UACC-62 melanoma cell clones (KO#28 and KO#31) previously generated in our lab using CRISPR-Cas9 technology (Fig. 2B). As shown in Supplementary Figure 2, UACC-62 is a suitable *in vitro* model to study MITF, as it shows detectable levels of the protein, which is mainly located in the nucleus. Importantly, both TRIB2-deficient clones displayed significantly reduced mRNA (Fig. 2C) and protein levels (Fig. 2D) of MITF compared to WT UACC-62 cells. In addition, consistent with reduced MITF activity, qPCR analysis revealed decreased expression of MITF target genes involved in melanin synthesis and melanosome structure (PMEL, MLANA, TYR, TYRP1) in TRIB2 KO cells (Fig. 2E). DCT mRNA was paradoxically increased in KO cells (Fig. 2E). Finally, as high adhesion capacity is a well-established phenotypic characteristic of differentiated melanoma cells [26], we wondered whether TRIB2 removal also affected the ability of UACC-62 cells to adhere to fibronectin. Fibronectin adhesion assays

showed that TRIB2 KO clones had a significantly lower capacity to adhere compared to parental UACC-62 cells (Fig. 2F).

In summary, our *in vitro* experiments support the hypothesis that TRIB2 maintains the differentiated status in melanoma, acting as an upstream modulator of MITF and the melanogenic transcription program.

TRIB2 maintains β-catenin expression and restrains a WNT5A/NFATC2-associated program in melanoma

WNT signaling pathways are related to phenotype switching in melanoma, as they mediate both melanocytic lineage commitment or migration by controlling MITF activity and actin cytoskeleton [27]. Canonical β-catenin-dependent pathway and non-canonical WNT/Ca^{2+} signaling have been associated to opposite melanoma cell states, being linked to the differentiated/pigmented and the invasive/dedifferentiated phenotype, respectively [11]. Then, to broaden our understanding about how TRIB2 sustains a melanocytic identity in melanoma, we next focused on both WNT signaling pathways.

As shown in Fig. 3A, a moderate-strength Pearson correlation between TRIB2 and CTNNB1 was observed in tumors from the TCGA-SKCM dataset. Supporting this association between TRIB2 and CTNNB1 in melanoma, positive Pearson correlations between TRIB2 and CTNNB1 were also observed in tumors from the Liu et al. (2019) and Riaz et al. (2017) cohorts, as well as in malignant cells from the Jerby-Arnon et al. (2018) dataset (Supplementary Fig. 3A, 3B and 3C). Next, to clarify whether there was a causal relationship between TRIB2 and CTNNB1/β-catenin, we leveraged our TRIB2 KO UACC-62 cellular model. TRIB2-deficient clones displayed a diminished mRNA expression of CTNNB1 compared to WT UACC-62 cells, as determined by qPCR (Fig. 3B). Accordingly, WB analyses showed significantly decreased protein levels of β-catenin in TRIB2 KO clones (Fig. 3C). To explore whether TRIB2 also modulates β-catenin subcellular location, immunofluorescence experiments were performed. However, we found a global reduction of β-catenin mean fluorescence intensity (MFI) in TRIB2 KO clones rather than a different distribution of the fluorescence between cytoplasm and nucleus when compared to parental UACC-62 cells (Fig. 3D). To evaluate whether β-catenin reduction in the absence of TRIB2 leads to a decrease in the expression of its target genes, we measured CCND1 and CCND2 as readouts using qPCR. As shown by Fig. 3E, both CCND1 and CCND2 were significantly decreased in TRIB2 KO clones.

To next investigate WNT/Ca^{2+} pathway, we first conducted correlation analysis in the TCGA-SKCM cohort between TRIB2 and the ligand of the pathway, WNT5A. As a result, we found a weak but significant negative correlation between TRIB2 and WNT5A (Fig. 3F). Importantly, qPCR analyses revealed that TRIB2 KO clones had increased levels of genes involved in the WNT/Ca^{2+} pathway: WNT5A, PLCB1 and the transcription factor NFATC2 (Fig. 3G). In line with these observations, NFATC2 protein was readily detected in TRIB2-deficient clones but remained undetectable in WT UACC-62 cells (Fig. 3H).

Finally, we examined SFRP1, a secreted modulator of WNT signaling. SFRP1 expression was increased following TRIB2 depletion in UACC-62 cells; however, pharmacological inhibition of SFRP1 did not restore β-catenin levels in TRIB2-deficient cells (Supplementary Fig. 4), arguing against SFRP1 as a primary mediator of the reduced β-catenin abundance associated with TRIB2 loss.

In summary, these results indicate that TRIB2 maintains β-catenin expression while restraining WNT5A-NFATC2, providing additional evidence of the role of TRIB2 as a mediator of the melanocytic identity in melanoma.

TRIB2 sustains the melanogenic response to canonical WNT signaling

To further investigate the relationship between TRIB2, canonical WNT pathway and the melanogenic program, we wondered whether TRIB2 expression influences the response of melanoma cells to pharmacological or ligand-mediated activation of the WNT/β-catenin pathway. To this end, we treated WT and TRIB2 KO UACC-62 cells with conditioned media containing the canonical ligand WNT3A or the GSK3β inhibitor CHIR98014 for 48 h (Fig. 4A). Both treatments significantly increased total β-catenin protein in WT and TRIB2-deficient cells, but the greatest levels were observed in parental UACC-62 cells (Fig. 4B), suggesting that TRIB2 is needed for the highest accumulation of β-catenin in response to canonical pathway stimulation. Furthermore, we also measured by qPCR the expression of MITF and the melanogenic genes that were reduced upon TRIB2 depletion: PMEL, MLANA, TYR and TYRP1. Considering all these genes as a whole, we found that, similar to β-catenin, the highest expression of the melanogenic program was observed in UACC-62 TRIB2 WT cells following WNT/β-catenin pathway activation (Fig. 4C).

In sum, this data indicates that TRIB2 is mediating the induction of the MITF-dependent melanogenic program by β-catenin, contributing to the full melanogenic response to canonical WNT signaling.

TRIB2 co-expression signature stratifies melanoma patients into groups with distinct survival outcomes and differentiation status

Having established that TRIB2 causally sustains the MITF- and β-catenin-dependent differentiation program *in vitro*, we next asked whether this transcriptional axis also carries prognostic value in melanoma patients. To this end, we used top positively and top negatively co-expressed genes identified in Figure 1 together with TRIB2 to perform K-means clustering of TCGA-SKCM patients into two groups (Fig. 5A). As a result, two well-defined groups were obtained after running the K-means clustering algorithm, visualized on a PCA plot where PC1 and PC2 accounted for 28.1% and 6.6% of the variance, respectively (Fig. 5B). Importantly, Cluster 2 showed a lower overall survival, as determined by a log-rank test ($p = 0.042$) (Fig. 5C), and a significant higher expression of TRIB2 compared to Cluster 1 (Fig. 5D). Moreover, and according to their dependence on TRIB2 expression, MITF and MITF target genes related to melanocytic pigmentation, as well as CTNNB1, were also increased in tumors from Cluster 2 (Fig. 5D). Conversely, WNT5A was reduced in Cluster 2 (Fig. 5D).

Overall, these data show that stratification of melanoma patients based on the TRIB2 transcriptomic landscape identifies individuals with differential prognosis, and supports a potential role for TRIB2 as a candidate prognostic biomarker in melanoma. Additionally, they also suggest that high-TRIB2 tumors are defined by a differentiation/pigmentation phenotype.

TRIB2 is associated with a $CD8^+$ T cell evasion phenotype and increased expression in immunoresistant melanoma cells

It is widely recognized that $CD8^+$ cytotoxic T cells play a crucial role in anti-tumor immunity, and that mechanisms acquired by melanoma cells to evade $CD8^+$ T cell cytotoxic activity contribute to ICI resistance [28]. As TRIB2 top negatively correlated genes identified in Figure 1 were related to immune system activation, we hypothesized that a negative association between TRIB2 and $CD8^+$ T cell activity could provide additional information about the poorer prognosis of high-TRIB2 tumors from Cluster 2. To address this, we analyzed the correlation of TRIB2 with a specific $CD8^+$ T cell gene signature (CD8A, CD8B, GZMA, GZMB, PRF1, IFNG, CCL5, CXCL9, CXCL10, LAG3) in TCGA-SKCM patients. TRIB2 showed weak but significant negative Pearson correlations with all $CD8^+$ T cell genes considered (Fig. 6A). Moreover, when the expression of $CD8^+$-related genes was analyzed in the clusters based on the TRIB2 co-expression signature, we found that all of them were significantly decreased in Cluster 2 (Fig. 6B), suggesting that high-TRIB2 tumors are characterized by reduced $CD8^+$ T cell-related gene expression and supporting a potential link between TRIB2 expression and CD8+ T cell evasion mechanisms in melanoma.

Furthermore, we investigated whether TRIB2 expression was associated with resistance to ICI. To this end, we analyzed TRIB2 expression in tumor samples from the Liu et al. (2019) [23] and Riaz et al. (2017) [24] cohorts (Fig. 6C). In pretreatment tumor samples from the Liu et al. cohort, TRIB2 expression was significantly higher in patients who did not derive clinical benefit from anti-PD1 therapy (Fig. 6D). Consistently, in the Riaz et al. cohort, TRIB2 expression remained unchanged during anti-PD1 treatment in non-responders, whereas it decreased in on-treatment tumors from responding patients relative to their matched pretreatment samples (Fig. 6E).

Together, these findings suggest that elevated TRIB2 expression, beyond sustaining a differentiated identity, is linked to $CD8^+$ T cell evasion and resistance to anti-PD1 therapy in melanoma.

Discussion

In this study, we uncover a novel role of TRIB2 as a modulator of melanoma cell plasticity, identifying TRIB2 as a key protein for maintaining the differentiated phenotype of melanoma cells. Leveraging publicly available RNAseq datasets from melanoma patients and our TRIB2 KO genetic *in vitro* model, we found that TRIB2 regulates three main processes related to the melanocytic identity: the sustaining of

MITF-related melanogenic program, the maintenance of β-catenin-dependent signaling and the restraining of key elements belonging to the WNT/Ca^{2+} pathway.

These three pathways we have shown here to be regulated by TRIB2 are tightly interconnected and act coordinately to define the phenotype of melanoma tumors. It has been described that canonical WNT/β-catenin and non-canonical WNT/Ca^{2+} pathways are reciprocally antagonized, triggering mutually exclusive programs that underlie melanoma cell identity by controlling melanocytic commitment, cytoskeleton rearrangement and cellular motility [27]. Both β-catenin and WNT5A signaling have been proposed to modulate the MITF transcription program but in an opposite way. Whereas WNT5A inhibits the induction of MITF transcription by PAX3 [29], WNT/β-catenin positively modulates MITF activity at different levels. It is described that β-catenin/LEF complexes contribute to both the induction of MITF expression and the transcription of melanogenic genes as cofactors for MITF [30,31]. Additionally, it has been also reported that WNT3A, through the inhibition of GSK3β, increases the stability of MITF protein [32]. Regarding TRIB2, different cancer investigations have been focused on the relation between TRIB2 and β-catenin so far, and a context-dependent reciprocal regulation can be inferred from all these studies [33-38]. In our TRIB2 KO *in vitro* model, we observed a reduction of β-catenin at the mRNA and protein level. Moreover, we show that TRIB2 expression is necessary for both the highest accumulation of β-catenin and a full melanogenic response to the WNT canonical pathway activation, which in the context of patients would imply a higher sensitivity of high TRIB2 tumors to develop a differentiated identity in response to WNT/β-catenin activation. In any case, despite the results of this set of experiments, it is unlikely that TRIB2 acts as an upstream regulator of a straightforward axis responsible for the melanogenic phenotype. Because of its role as a scaffold protein, TRIB2 works as an intracellular platform that brings together proteins from different pathways, including C/EBPα, COP1, MEK, Smurf1 and others [15,39-41], integrating signals that trigger different cellular responses. Therefore, due to the interconnected nature of the three pathways and the capacity of TRIB2 to orchestrate complex signaling networks, TRIB2 may be modulating them at various levels that ultimately result in the observed phenotype.

Although the results we have obtained in our TRIB2 KO UACC-62 model are robust and consistent with available literature, we are aware that the inclusion of a single melanoma cell line in the study is the main limitation of our research. However, we supported our *in vitro* findings by showing the association of TRIB2 with the melanocytic identity in four different RNAseq cohorts including patients with distinct phenotypes and treatments, which highlights the relevance of TRIB2 as a modulator of the melanoma cell biology.

Beyond the role of TRIB2 in melanogenic differentiation, we have associated TRIB2 expression in melanoma with immune evasion and immunoresistance for the first time. Leveraging publicly available cohorts of melanoma patients subjected to anti-PD1 therapy, we found two main lines of evidence: first, that TRIB2 expression was already increased in tumors from patients without clinical benefit following treatment; second, that TRIB2 diminished during treatment in tumors from responder patients while

remaining unchanged in non-responders. Importantly, the stratification of TCGA-SKCM melanoma patients based on our TRIB2 coexpression signature allowed us to clearly define a group of patients with poor prognosis whose tumors were characterized by high levels of TRIB2, MITF and CTNNB1, but diminished levels of WNT5A and $CD8^+$-related genes. Thus, our data links the TRIB2-sustained differentiated phenotype to a lower $CD8^+$ T cell-related gene expression in these tumors. Currently, how melanoma cell identity influences immune surveillance and response to immunotherapy is still a matter of discussion. Evidence supporting the more immunogenic nature of both dedifferentiated and differentiated phenotype has been reported [6,42-44]. In line with our findings, it has been previously shown that high-grade melanomas displayed an increased expression of MITF and its target genes TYR and MLANA, whereas expressing an inverse pattern of immune-related genes CD3E, CD3D, and LCK [45]. Accordingly, the silencing of MITF in human melanoma cell lines leads to increased chemokine release and immune cell attraction, while overexpression of MITF led to lower immune cell attraction [46]. Moreover, scRNAseq of melanoma biopsies unveiled that T cell infiltration was positively correlated with factors expressed by CAFs and that the expression of a $MITF^{high}$ program in melanoma cells was negatively correlated with CAF abundance and T cell infiltration [47]. In parallel to MITF, the canonical β-catenin-dependent pathway has also been associated to a reduced infiltration of T cell in melanoma tumors, and tumor-intrinsic activation of β-catenin has been proposed to be a mechanism of resistance to ICI therapy [12]. Since we have established associations between TRIB2 and immune resistance, rather than a causal relationship, further research is needed to elucidate the exact role of TRIB2 in these processes. However, we cannot rule out that TRIB2, through the MITF program, β-catenin, or other genes may be responsible for the reduction in immunogenicity in melanoma. Indeed, it was recently described that TRIB2 epigenetically inhibits genes related to antigen presentation and T-cell recruitment in glioblastoma [48]. Therefore, there is precedent for TRIB2 as a regulator of immune evasion in other tumor types, supporting its plausibility as a mediator of immunoresistance in melanoma as well.

In summary, our findings identify TRIB2 as a coordinator of the programs that underlie the melanogenic identity of melanoma cells, positioning TRIB2 as a novel modulator of phenotype switching in melanoma. Furthermore, the current data suggest a potential role of TRIB2 in T cell exclusion and resistance to ICI. Our work expands current understanding of TRIB2 as a regulator of cellular processes in melanoma, providing new evidence on the mechanisms that melanoma tumors could exploit to escape advanced therapies.

Declarations

Acknowledgements

Not applicable.

Conflict of Interest

Wolfgang Link is a co-founder of Refoxy Pharmaceuticals GmbH, Cologne, Germany, and declares this potential conflict of interest in accordance with the requirements of his institution. The remaining authors have no conflicts of interest to declare.

Author contribution

Conceived and designed the study: A.d.R.-M., A.O.-S., L.J. and W.L. Performed all the experiments and analyzed the data: A.d.R.-M., A.O.-S. and L.J. with the support of A.R.-M., I.V.-M. and S.C.-S. Provided reagents, protocols and materials: M.J.M.-B., P.B., A.B., A.F.-B., B.I.F. and W.L. Interpreted and discussed the data: A.d.R.-M., A.O.-S., L.J., B.I.F. and W.L. Wrote the paper: A.d.R.-M., A.O.-S., L.J. and W.L. All authors read and approved the final paper.

Funding Statement

This work was supported by a grant to Wolfgang Link from the Spanish Ministerio de Ciencia e Innovación/Agencia Estatal de Investigación and the European Regional Development Fund (PID2022-136654OB-I00, financed by MCIN/AEI/10.13039/501100011033/FEDER, UE), and by a grant to Bibiana I. Ferreira from the Fundação para a Ciência e a Tecnologia (FCT, grant PTDC/MED-ONC/4167/2020) and the Algarve Biomedical Center (ABC).

Availability of Data and Materials

The data in this study will be made available from the lead contact upon request.

References

1. Tasdogan, A. *et al.* Cutaneous melanoma. *Nature Reviews Disease Primers***11**, doi:10.1038/s41572-025-00603-8 (2025).
2. Zheng, D. X. *et al.* Overcoming Resistance Mechanisms to Melanoma Immunotherapy. *American Journal of Clinical Dermatology***26**, 77-96, doi:10.1007/s40257-024-00907-7 (2024).
3. Centeno, P. P., Pavet, V. & Marais, R. The journey from melanocytes to melanoma. *Nature Reviews Cancer***23**, 372-390, doi:10.1038/s41568-023-00565-7 (2023).
4. Kuras, M. Exploring the Complex and Multifaceted Interplay between Melanoma Cells and the Tumor Microenvironment. *International Journal of Molecular Sciences***24**, 14403, doi:10.3390/ijms241814403 (2023).
5. Benboubker, V., Boivin, F., Dalle, S. & Caramel, J. Cancer Cell Phenotype Plasticity as a Driver of Immune Escape in Melanoma. *Frontiers in Immunology***13**, doi:10.3389/fimmu.2022.873116 (2022).
6. Hossain, S. M. & Eccles, M. R. Phenotype Switching and the Melanoma Microenvironment; Impact on Immunotherapy and Drug Resistance. *International Journal of Molecular Sciences***24**, 1601, doi:10.3390/ijms24021601 (2023).

7. Hartman, M. L. & Czyz, M. MITF in melanoma: mechanisms behind its expression and activity. *Cellular and Molecular Life Sciences***72**, 1249-1260, doi:10.1007/s00018-014-1791-0 (2014).
8. Vera, O. *et al.* A MAFG~MITF complex drives melanoma phenotype switching and progression. *Nature Communications***17**, doi:10.1038/s41467-026-73291-x (2026).
9. Arozarena, I. & Wellbrock, C. Phenotype plasticity as enabler of melanoma progression and therapy resistance. *Nature Reviews Cancer***19**, 377-391, doi:10.1038/s41568-019-0154-4 (2019).
10. Webster, M. R., Kugel, C. H. & Weeraratna, A. T. The Wnts of change: How Wnts regulate phenotype switching in melanoma. *Biochimica et Biophysica Acta (BBA) - Reviews on Cancer***1856**, 244-251, doi:10.1016/j.bbcan.2015.10.002 (2015).
11. Gajos-Michniewicz, A. & Czyz, M. WNT Signaling in Melanoma. *International Journal of Molecular Sciences***21**, 4852, doi:10.3390/ijms21144852 (2020).
12. Spranger, S., Bao, R. & Gajewski, T. F. Melanoma-intrinsic β-catenin signalling prevents anti-tumour immunity. *Nature***523**, 231-235, doi:10.1038/nature14404 (2015).
13. Link, W. Tribbles breaking bad: TRIB2 suppresses FOXO and acts as an oncogenic protein in melanoma. *Biochemical Society Transactions***43**, 1085-1088, doi:10.1042/bst20150102 (2015).
14. Ferreira, B. I., Santos, B., Link, W. & De Sousa-Coelho, A. L. Tribbles Pseudokinases in Colorectal Cancer. *Cancers***13**, 2825, doi:10.3390/cancers13112825 (2021).
15. Mayoral-Varo, V., Jiménez, L. & Link, W. The Critical Role of TRIB2 in Cancer and Therapy Resistance. *Cancers***13**, 2701, doi:10.3390/cancers13112701 (2021).
16. Hannon, M. M. *et al.* Elevated TRIB2 with NOTCH1 activation in paediatric/adult T-ALL. *British Journal of Haematology***158**, 626-634, doi:10.1111/j.1365-2141.2012.09222.x (2012).
17. Wei, G., Lu, T., Shen, J. & Wang, J. LncRNA ZEB1-AS1 promotes pancreatic cancer progression by regulating miR-505-3p/TRIB2 axis. *Biochemical and Biophysical Research Communications***528**, 644-649, doi:10.1016/j.bbrc.2020.05.105 (2020).
18. Wang, J. *et al.* Impaired Phosphorylation and Ubiquitination by p70 S6 Kinase (p70S6K) and Smad Ubiquitination Regulatory Factor 1 (Smurf1) Promote Tribbles Homolog 2 (TRIB2) Stability and Carcinogenic Property in Liver Cancer. *Journal of Biological Chemistry***288**, 33667-33681, doi:10.1074/jbc.M113.503292 (2013).
19. Kritsch, D. *et al.* Tribbles 2 mediates cisplatin sensitivity and DNA damage response in epithelial ovarian cancer. *International Journal of Cancer***141**, 1600-1614, doi:10.1002/ijc.30860 (2017).
20. Miyanaga, A. *et al.* Whole-exome and RNA sequencing of pulmonary carcinoid reveals chromosomal rearrangements associated with recurrence. *Lung Cancer***145**, 85-94, doi:10.1016/j.lungcan.2020.03.027 (2020).
21. Hill, R. *et al.* TRIB2 as a biomarker for diagnosis and progression of melanoma. *Carcinogenesis***36**, 469-477, doi:10.1093/carcin/bgv002 (2015).
22. Jerby-Arnon, L. *et al.* A Cancer Cell Program Promotes T Cell Exclusion and Resistance to Checkpoint Blockade. *Cell***175**, 984-997.e924, doi:10.1016/j.cell.2018.09.006 (2018).

23. Liu, D. *et al.* Integrative molecular and clinical modeling of clinical outcomes to PD1 blockade in patients with metastatic melanoma. *Nature Medicine***25**, 1916-1927, doi:10.1038/s41591-019-0654-5 (2019).
24. Riaz, N. *et al.* Tumor and Microenvironment Evolution during Immunotherapy with Nivolumab. *Cell***171**, 934-949.e916, doi:10.1016/j.cell.2017.09.028 (2017).
25. Machado, S. *et al.* Harmine and Piperlongumine Revert TRIB2-Mediated Drug Resistance. *Cancers***12**, 3689, doi:10.3390/cancers12123689 (2020).
26. Pillai, M. *et al.* Mapping phenotypic heterogeneity in melanoma onto the epithelial-hybrid-mesenchymal axis. *Frontiers in Oncology***12**, doi:10.3389/fonc.2022.913803 (2022).
27. Arozarena, I. & Wellbrock, C. Targeting invasive properties of melanoma cells. *The FEBS Journal***284**, 2148-2162, doi:10.1111/febs.14040 (2017).
28. Raskov, H., Orhan, A., Christensen, J. P. & Gögenur, I. Cytotoxic CD8+ T cells in cancer and cancer immunotherapy. *British Journal of Cancer***124**, 359-367, doi:10.1038/s41416-020-01048-4 (2020).
29. Dissanayake, S. K. *et al.* Wnt5A Regulates Expression of Tumor-Associated Antigens in Melanoma via Changes in Signal Transducers and Activators of Transcription 3 Phosphorylation. *Cancer Research***68**, 10205-10214, doi:10.1158/0008-5472.can-08-2149 (2008).
30. Widlund, H. R. *et al.* β-Catenin–induced melanoma growth requires the downstream target Microphthalmia-associated transcription factor. *The Journal of Cell Biology***158**, 1079-1087, doi:10.1083/jcb.200202049 (2002).
31. Takeda, K. *et al.* Induction of Melanocyte-specific Microphthalmia-associated Transcription Factor by Wnt-3a. *Journal of Biological Chemistry***275**, 14013-14016, doi:10.1074/jbc.C000113200 (2000).
32. Ploper, D. *et al.* MITF drives endolysosomal biogenesis and potentiates Wnt signaling in melanoma cells. *Proceedings of the National Academy of Sciences***112**, doi:10.1073/pnas.1424576112 (2015).
33. Wang, J. *et al.* TRIB2 Acts Downstream of Wnt/TCF in Liver Cancer Cells to Regulate YAP and C/EBPα Function. *Molecular Cell***51**, 211-225, doi:10.1016/j.molcel.2013.05.013 (2013).
34. Xu, S. *et al.* TRIB2 inhibits Wnt/β-Catenin/TCF4 signaling through its associated ubiquitin E3 ligases, β-TrCP, COP1 and Smurf1, in liver cancer cells. *FEBS Letters***588**, 4334-4341, doi:10.1016/j.febslet.2014.09.042 (2014).
35. Chen, Z. *et al.* Knockdown of circ_0084043 suppresses the development of human melanoma cells through miR-429/tribbles homolog 2 axis and Wnt/β-catenin pathway. *Life Sciences***243**, 117323, doi:10.1016/j.lfs.2020.117323 (2020).
36. Wang, N., Wen, J., Ren, W., Wu, Y. & Deng, C. Upregulation of TRIB2 by Wnt/β-catenin activation in BRAFV600E papillary thyroid carcinoma cells confers resistance to BRAF inhibitor vemurafenib. *Cancer Chemotherapy and Pharmacology***88**, 155-164, doi:10.1007/s00280-021-04270-w (2021).
37. Liu, Q. *et al.* Long noncoding RNA TUG1 regulates the progression of colorectal cancer through miR-542-3p/TRIB2 axis and Wnt/β-catenin pathway. *Diagnostic Pathology***16**, doi:10.1186/s13000-021-01101-7 (2021).

38. Kim, D. K. *et al.* TRIB2 Stimulates Cancer Stem-Like Properties through Activating the AKT-GSK3β-β-Catenin Signaling Axis. *Molecules and Cells***44**, 481-492, doi:10.14348/molcells.2021.0030 (2021).
39. Liu, Y.-R. *et al.* Oncogenic TRIB2 interacts with and regulates PKM2 to promote aerobic glycolysis and lung cancer cell procession. *Cell Death Discovery***8**, doi:10.1038/s41420-022-01095-1 (2022).
40. Liu, W. *et al.* E3 ubiquitin ligase Smurf1 promotes cardiomyocyte pyroptosis by mediating ubiquitin-dependent degradation of TRIB2 in a rat model of heart failure. *International Reviews of Immunology***44**, 165-179, doi:10.1080/08830185.2024.2434058 (2025).
41. Warma, A., Lussier, J. G. & Ndiaye, K. Tribbles Pseudokinase 2 (TRIB2) Regulates Expression of Binding Partners in Bovine Granulosa Cells. *International Journal of Molecular Sciences***22**, 1533, doi:10.3390/ijms22041533 (2021).
42. Riesenberg, S. *et al.* MITF and c-Jun antagonism interconnects melanoma dedifferentiation with pro-inflammatory cytokine responsiveness and myeloid cell recruitment. *Nature Communications***6**, doi:10.1038/ncomms9755 (2015).
43. Thier, B. *et al.* Innate immune receptor signaling induces transient melanoma dedifferentiation while preserving immunogenicity. *Journal for ImmunoTherapy of Cancer***10**, e003863, doi:10.1136/jitc-2021-003863 (2022).
44. Ando, Y. *et al.* Hyperdifferentiated murine melanoma cells promote adaptive anti-tumor immunity but activate the immune checkpoint system. *OncoImmunology***14**, doi:10.1080/2162402x.2024.2437211 (2024).
45. Harbst, K. *et al.* Molecular Profiling Reveals Low- and High-Grade Forms of Primary Melanoma. *Clinical Cancer Research***18**, 4026-4036, doi:10.1158/1078-0432.ccr-12-0343 (2012).
46. Wiedemann, G. M. *et al.* Microphthalmia-Associated Transcription Factor (MITF) Regulates Immune Cell Migration into Melanoma. *Translational Oncology***12**, 350-360, doi:10.1016/j.tranon.2018.10.014 (2019).
47. Tirosh, I. *et al.* Dissecting the multicellular ecosystem of metastatic melanoma by single-cell RNA-seq. *Science***352**, 189-196, doi:10.1126/science.aad0501 (2016).
48. Segura-Collar, B. *et al.* The TRIB2–DNMT1 Pathway Generates an Immune-Cold Microenvironment in Glioblastoma, and Its Inhibition Promotes Immunotherapy. *Cancer Immunology Research***13**, 1022-1036, doi:10.1158/2326-6066.cir-24-0807 (2025).

Figures

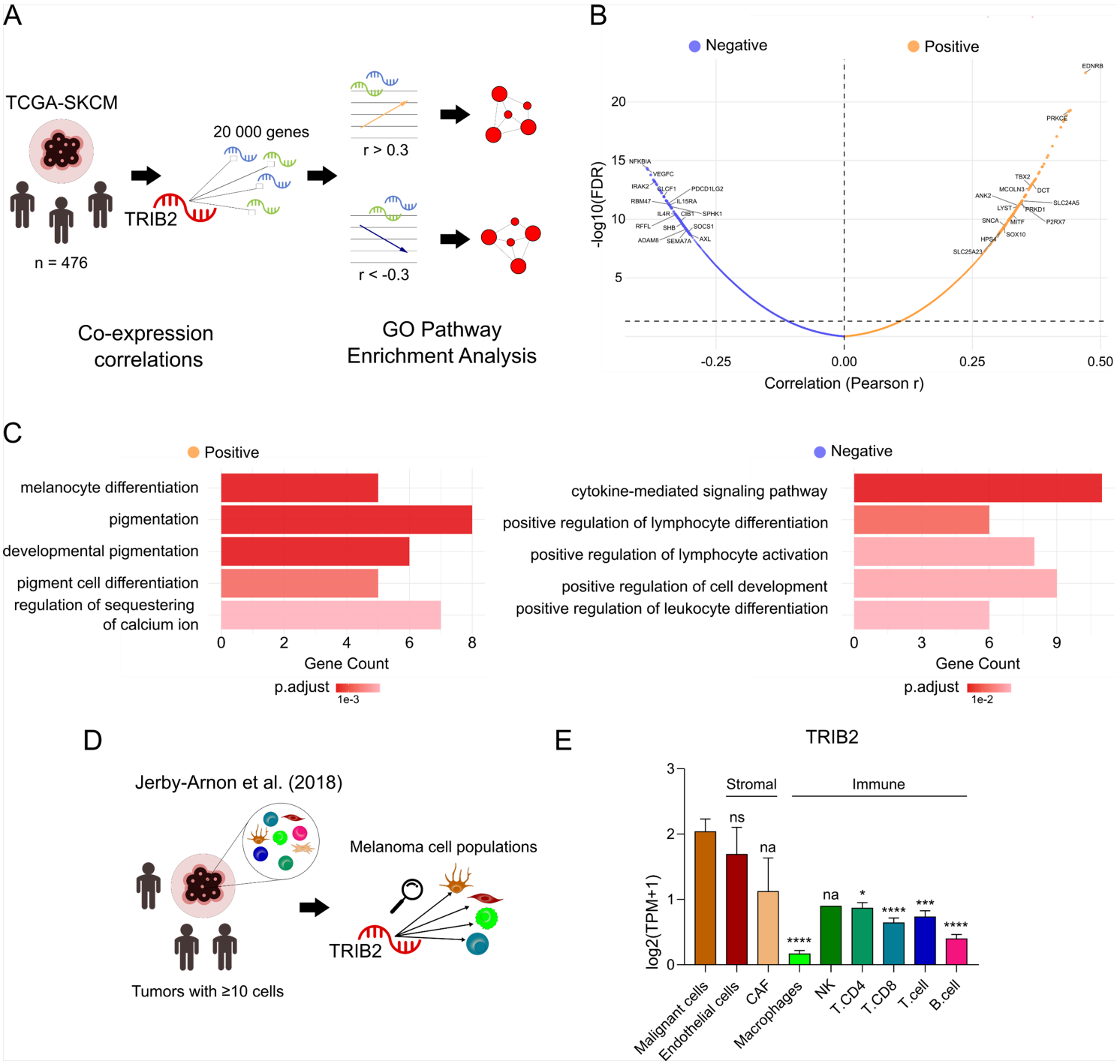


Figure 1

TRIB2 co-expression analysis in melanoma reveals associations with melanocyte differentiation and immune-related pathways. A Schematic overview of the co-expression analysis pipeline. Pearson correlation coefficients between TRIB2 and ~20 000 genes were computed in the TCGA-SKCM cohort (n = 476). Genes with r > 0.3 (top positively co-expressed genes) or r < −0.3 (top negatively co-expressed genes) were selected and subjected to GO Pathway Enrichment Analysis. **B** Volcano plot of Pearson correlation coefficients (x-axis) versus −log10(FDR) (y-axis) for all genes co-expressed with TRIB2 in TCGA-SKCM. TRIB2 positively and negatively correlated genes are highlighted in red and blue respectively. Genes associated with the top 5 enriched GO biological processes among the top positively

and negatively TRIB2-coexpressed genes are labeled. **C** Bar plots showing the top 5 enriched GO biological process terms among TRIB2 top positively co-expressed genes (left) and top negatively co-expressed genes (right). Bar size represents gene count and color indicates adjusted p-value. **D** Schematic representation of the analytical workflow followed to examine TRIB2 expression across melanoma cell populations annotated in the scRNA-seq dataset from Jerby-Arnon et al. (2018). TRIB2 expression was averaged across cells of each population within every individual tumor (pseudobulk approach). Only tumor–population combinations comprising at least 10 profiled cells were retained for analysis. **E** Bar graph showing TRIB2 expression [log2(TPM+1)] across distinct cell populations from the single-cell melanoma dataset from Jerby-Arnon et al (2018). NK and CAF populations were represented by fewer than three tumors; their means are shown for descriptive purposes only, and statistical comparison with malignant cells was not performed (na).

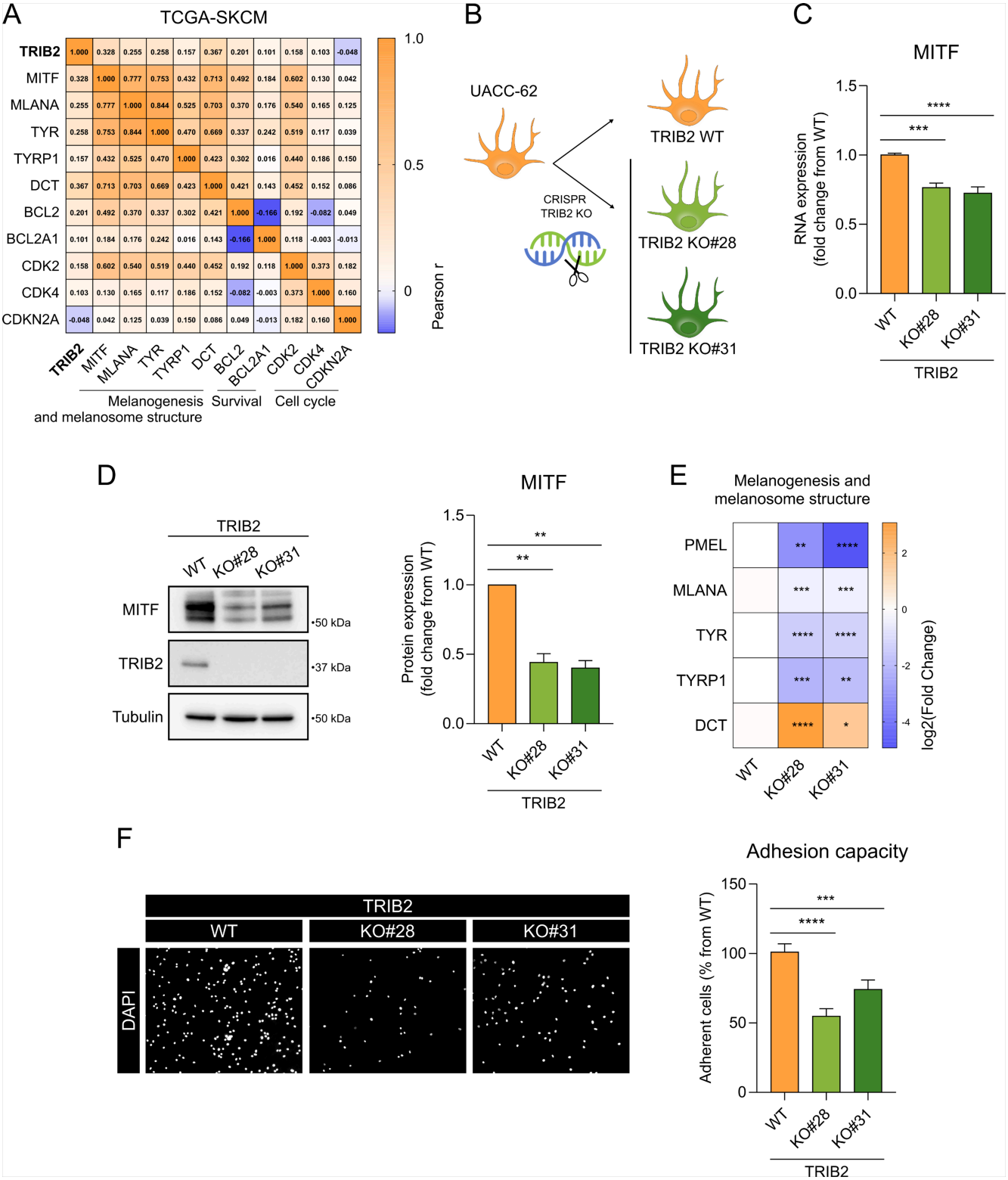


Figure 2

MITF transcription program depends on TRIB2 expression in melanoma. A Correlation matrix (Pearson r) between TRIB2 and the MITF gene program (MLANA, TYR, TYRP1, DCT, BCL2, BCL2A1, CDK2, CDK4, CDKN2A) across all TCGA-SKCM samples. **B** Schematic overview of the UACC-62 TRIB2 KO melanoma cell model. TRIB2 gene was deleted from the UACC-62 cell line using CRISPR-Cas9 technology and two TRIB2 KO clones were selected (KO#28 and KO#31). **C** RT-qPCR analysis of MITF mRNA expression in

WT UACC-62 and TRIB2 KO clones KO#28 and KO#31, expressed as fold change relative to TRIB2 WT UACC-62 cells (n = 10). **D** WB analyses of MITF and TRIB2 protein levels in WT UACC-62 and TRIB2 KO clones KO#28 and KO#31. Tubulin was used as a loading control (n = 9). **E** Heatmap showing the mRNA expression of MITF target genes related to melanogenesis and melanosome structure (PMEL, MLANA, TYR, TYRP1 and DCT) in WT UACC-62 and TRIB2 KO clones KO#28 and KO#31 as measured by RT-qPCR. mRNA expression is shown as log2(Fold Change from WT) (n = 5-8). **F**Fibronectin cell adhesion analyses performed with WT UACC-62 and TRIB2 KO clones KO#28 and KO#31. Adhesion capacity was quantified by counting DAPI-positive nuclei per field and is expressed as the percentage of adherent cells relative to WT UACC-62 cells (n = 4).

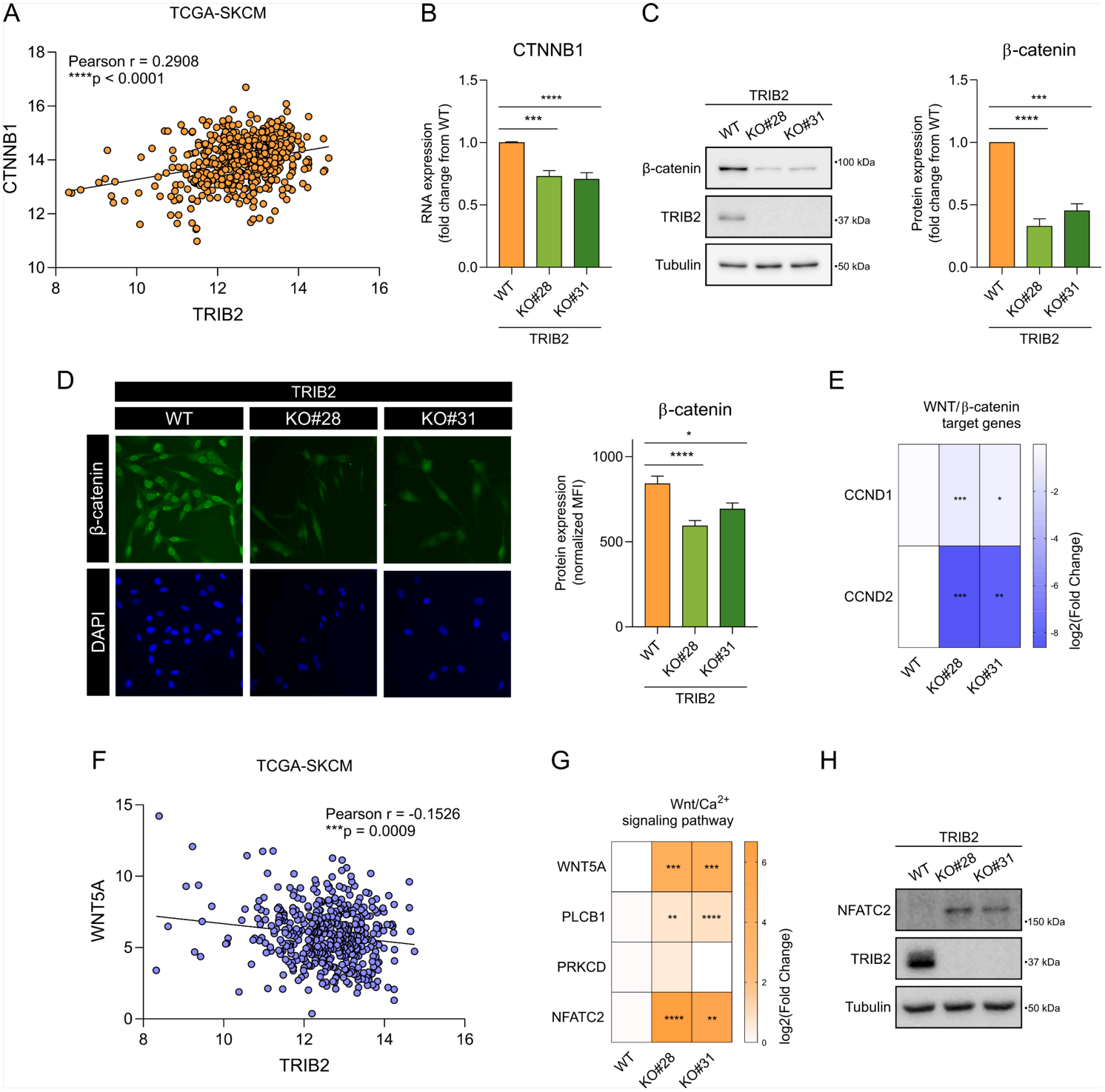


Figure 3

TRIB2 loss is accompanied by coordinated remodeling of WNT-associated signaling programs in UACC-62 cells. A Dot plot graph showing the correlation between TRIB2 and CTNNB1 in the TCGA-SKCM cohort. **B** RT-qPCR analysis of CTNNB1 mRNA expression in WT UACC-62 and TRIB2 KO clones KO#28 and KO#31, expressed as fold change relative to TRIB2 WT UACC-62 cells (n = 9). **C** WB analyses of β-catenin and TRIB2 protein levels in TRIB2 WT, KO#28, and KO#31 UACC-62 cells. Tubulin was used as a loading control (n = 13). **D** Immunofluorescence images of β-catenin (green) and DAPI nuclear staining (blue) in TRIB2 WT, KO#28, and KO#31 UACC-62 cells. Quantification of β-catenin immunofluorescence

signal expressed as normalized MFI is also shown (n = 4). **E** Heatmap showing the mRNA expression of WNT/ β-catenin target genes (CCND1, CCND2) in WT UACC-62 and TRIB2 KO clones KO#28 and KO#31 as measured by RT-qPCR. mRNA expression is shown as log2(Fold Change from WT) (n = 5). **F** Dot plot graph showing the correlation between TRIB2 and WNT5A in the TCGA-SKCM cohort. **G** Heatmap showing the mRNA expression of WNT/Ca^{2+} pathway components (WNT5A, PLCB1, PRKCD and NFATC2) in WT UACC-62 and TRIB2 KO clones KO#28 and KO#31 as measured by RT-qPCR. mRNA expression is shown as log2(Fold Change from WT) (n = 5). **H**Representative WB showing NFATC2 and TRIB2 protein levels in TRIB2 WT, KO#28, and KO#31 UACC-62 cells. Tubulin was used as a loading control (n = 3).

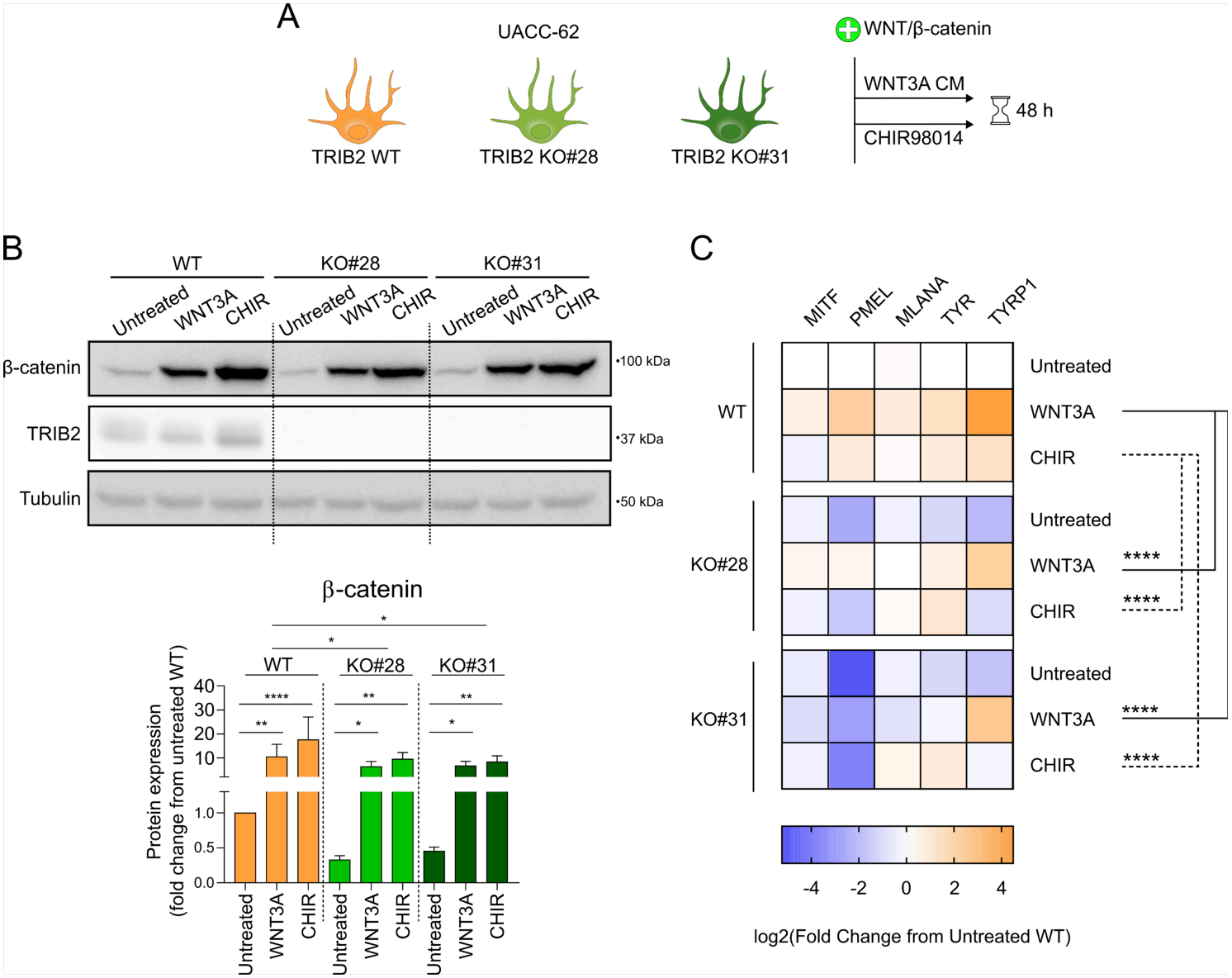


Figure 4

TRIB2 knockout impairs the induction of the melanogenic gene program by WNT/β-catenin signaling in UACC-62 cells. A Schematic overview of the WNT/β-catenin activation protocol in UACC-62 cells. WT UACC-62 and TRIB2 KO clones KO#28 and KO#31 were treated for 48 h with Wnt3a conditioned media or

the GSK3β inhibitor CHIR98014. **B** WB analyses of β-catenin and TRIB2 protein levels in TRIB2 WT, KO#28, and KO#31 UACC-62 cells after WNT/β-catenin signaling activation. Tubulin was used as a loading control (n = 3-13). **C**Heatmap showing the mRNA expression of MITF and related melanogenic genes in WT UACC-62 and TRIB2 KO clones KO#28 and KO#31 after WNT/β-catenin signaling activation as measured by RT-qPCR. mRNA expression is shown as log2(Fold Change from Untreated WT) (n = 5).

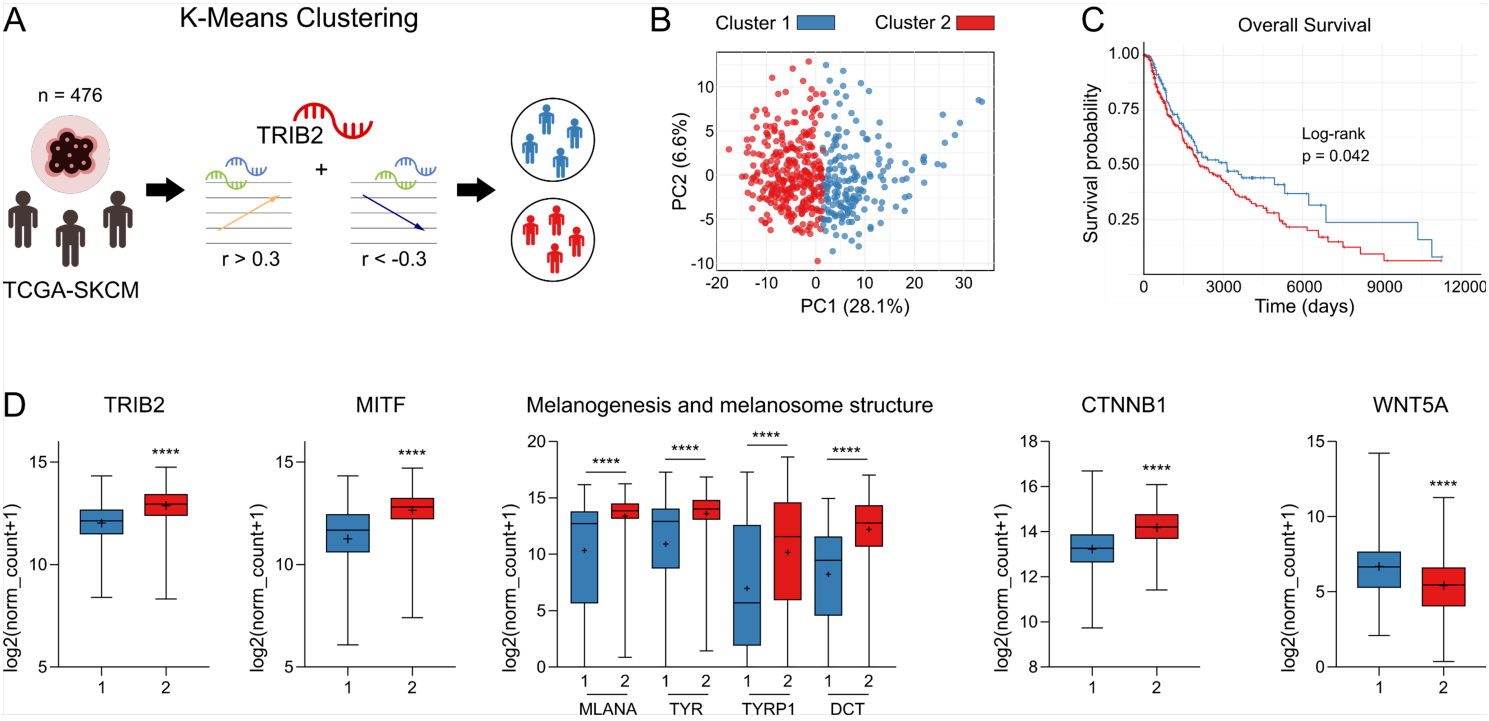


Figure 5

TRIB2 co-expression signature defines a differentiation-associated melanoma subgroup with reduced overall survival. A Schematic overview of the stratification of TCGA-SKCM patients based on TRIB2 co-expression landscape. The expression of TRIB2 and its top positively (Pearson r > 0.3) and negatively correlated genes (Pearson r < -0.3) was used to stratify patients into two distinct clusters by K-means clustering. **B** Principal Component Analysis (PCA) of TCGA-SKCM samples based on the expression of TRIB2 and its top positively and negatively correlated genes, showing PC1 (28.1%) and PC2 (6.6%). Samples are colored by K-means cluster assignment (Cluster 1 and Cluster 2). **C** Kaplan–Meier overall survival curves for TCGA-SKCM patients stratified in Cluster 1 and Cluster 2. **D** Box plot graph displaying the expression levels TRIB2, MITF, MITF target genes, CTNNB and WNT5A [log2(norm_count+1)] in Cluster 1 versus Cluster 2.

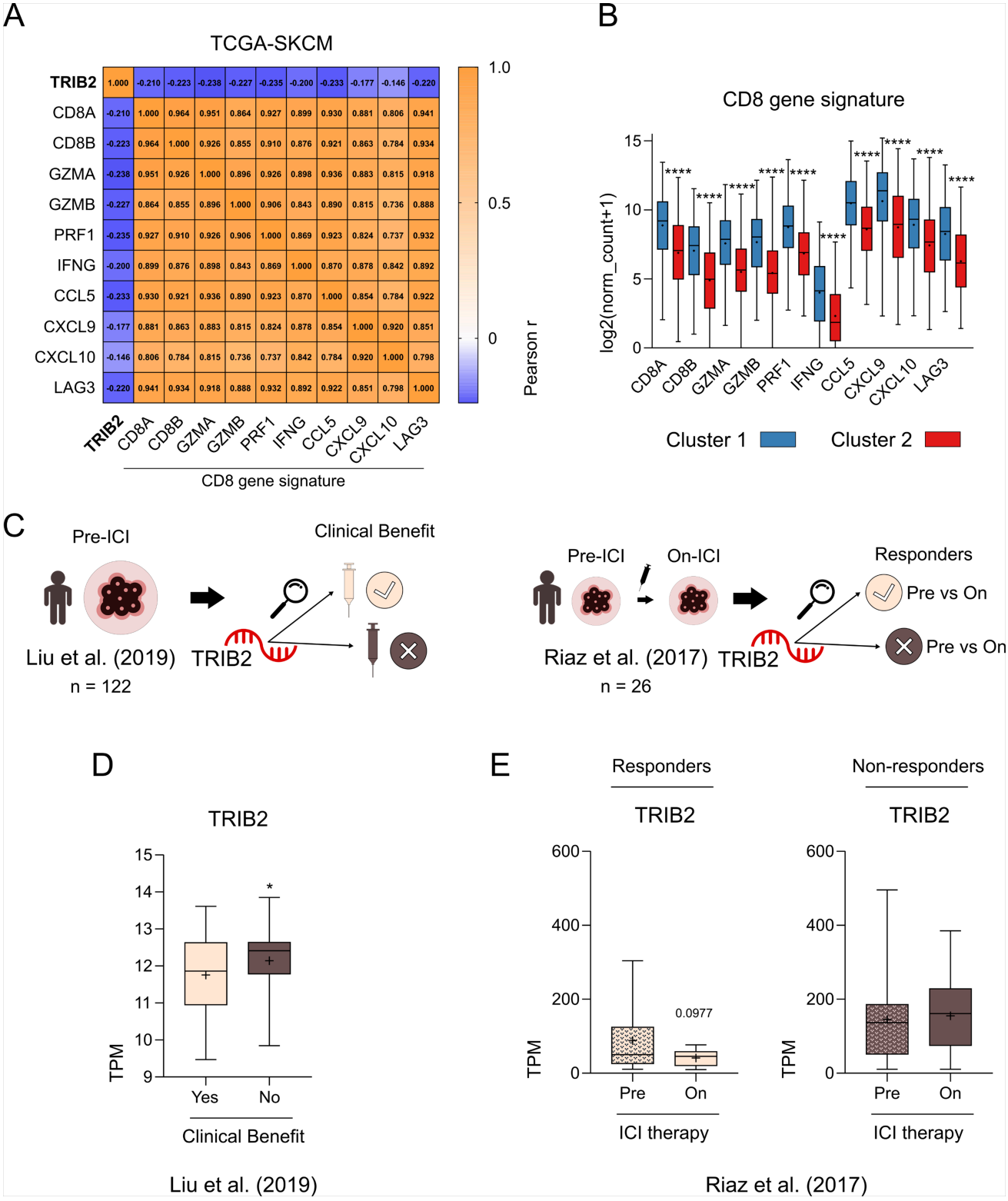


Figure 6

TRIB2 expression correlates with a CD8 T cell exclusion program and associates with an immunoresistant phenotype in melanoma. A Correlation matrix (Pearson r) between TRIB2 and the CD8 gene signature (CD8A, CD8B, GZMA, GZMB, PRF1, IFNG, CCL5, CXCL9, CXCL10, LAG3) across all TCGA-SKCM samples. **B** Box plot graph displaying the expression levels (log2[norm_count+1]) of representative genes composing the CD8 cytotoxic T cell gene signature in Cluster 1 versus Cluster 2. **C**

Schematic representation of the analyses performed in the Liu et al. (2019) and Riaz et al. (2017) melanoma cohorts to investigate the association between TRIB2 expression and immunoresistance. In the Liu et al. (2019) cohort, TRIB2 expression was evaluated in pre-treatment melanoma tumor samples from patients with or without clinical benefit following anti-PD1 therapy. In the Riaz et al. (2017) cohort, TRIB2 expression was assessed in tumor samples collected before treatment and during anti-PD1 therapy from responders and non-responders. **D** Bar graph showing TRIB2 expression (TPM) in pre-treatment melanoma samples from patients with positive or negative clinical benefit after anti-PD1 therapy. **E** Bar graphs showing TRIB2 expression (TPM) in pre-treatment and on-treatment melanoma samples from responders (left) and non-responders (right) receiving anti-PD1 therapy.

Supplementary Files

This is a list of supplementary files associated with this preprint. Click to download.

- delaRochaMuXXozSupplementaryFigures.pdf
- Supplementarymaterial1.xlsx